AMPLITUDE OF PcP, PcS, ScS, AND ScP IN DEEP-FOCUS EARTHQUAKES*

By KAZIM ERGIN

ABSTRACT

A systematic study has been made of the ratios of $\left(\frac{\text{displacement}}{\text{period}}\right)$ of PcP, PcS, ScS, and ScP to that of the corresponding incident wave $\left\{\text{e.g., } \left(\frac{\text{displacement}}{\text{period}}\right)_{PcP} \Big/ \left(\frac{\text{displacement}}{\text{period}}\right)_{P}\right\}$, using intermediate and deep-focus earthquake seismograms. The results indicate that the observed ratios of the horizontal components of the waves that are reflected as P waves (i.e., PcP/P and ScP/S) and that of the vertical component of the waves that are reflected as S waves (i.e., ScS/S and PcS/P) at the mantle-core boundary are considerably larger than the theoretical ones, whereas the observed ratios of the vertical component of the first group and that of the horizontal component of the second group are in fairly good agreement with the theoretical values. Theoretical computations were based on the assumption that in the case of a longitudinal wave the vibration is in the direction of propagation and in the case of a transverse wave the vibration is perpendicular to the direction of propagation. It is further found that the behavior of the direct P and S waves is in accord with the theory, but the vibration of the ground is not in the direction of propagation for PcP and ScP and is not perpendicular to the direction of propagation for PcS and ScS.

INTRODUCTION

THE PURPOSE of this work is to compare theoretical and observed ground displacements produced by PcP, PcS, ScS, and ScP, as well as direct P and S waves, upon their arrival at the surface of the earth, using seismograms of intermediate and deep-focus earthquakes that were recorded by standard seismographs at Pasadena. The same problem was treated by Martner [14],[1] who used Pasadena seismograms of shallow shocks ($h \leqq 60$ km.). He also used Dana's [2, 4] calculated values,[2] and compared them with his observational results. Dana had previously computed the theoretical ground displacements for P, SV, PcP, PcS, ScS, ScP, etc., as well as the displacement ratios of the waves reflected at the mantle-core boundary to that of the incident wave. His calculations were based on the formula given by Gutenberg [5, 6, 7], who had derived it from the original theory of Zoeppritz (Zoeppritz, Geiger, and Gutenberg [19]). The expression for the calculation of the ground displacement during a single body wave as a function of the epicentral distance is

$$KTN\sqrt{E_1} \tag{1}$$

where

$$N = Q\sqrt{(F_1F_2 \cdots F_n)\,\frac{\sin i_h di_h/d\Delta}{\sin \Delta \cos i_0}\,e^{-kD}} \tag{2}$$

In equation (2):

K is a constant depending on the fraction of the energy E_1 passing into the wave under consideration. It has three distinct values, for waves starting respectively as P, SH, and SV.

* Condensed from a Ph.D. dissertation at the California Institute of Technology. Manuscript received for publication July 5, 1950.

[1] Numbers in square brackets refer to the references listed at the end of this paper.

[2] Dana has assumed that $i_{os} = i_{op}$ for ScP and PcS. Therefore his values for these two waves are not correct and should be recalculated.

T is the period of the observed wave.

Q (or u/A_e, w/A_e) is the ratio of the horizontal and the vertical component of the total ground displacement (u and w respectively) to the amplitude of the incident wave.

F is the ratio of transmitted or reflected energy to incident energy at each point where the wave has encountered a discontinuity.

e^{-kD} is the absorption factor, where $k = 0.00012$/km. as given by Gutenberg [7] and D is the distance measured along the wave path.

i_h is the angle of incidence at the source at a depth h.

i_0 is the angle of incidence at the point of arrival at the surface.

Δ is the epicentral distance.

Since, previously, no theoretical values taking the depth of focus into account had been computed, the author has computed the theoretical values of N using the formula (2) for P, S, PcP, PcS, ScS, and ScP, for three different focal depths, namely, 100, 400, and 700 km.

When a P or S wave is incident at any discontinuity, the refracted and reflected S waves are of SV type, and when an SH wave is incident, it is reflected as SH wave only and no other type of wave is produced. But the direct S wave and ScS have both SV and SH components. The ratio SH/SV depends mainly on the mechanism of the shock and may have any value. To calculate the values of N for S and ScS, it was assumed that SH/SV = 1, i.e., the energy that passes into the S wave is divided equally between SV and SH. Since SH has no vertical component, any alternate assumption does not affect the value of N of the vertical component.

Calculated Values

Since in formula (1) K, T, and E_1 are not known, only N, which actually is

$$N = \frac{1}{K\sqrt{E_1}} \frac{u, w}{T}, \tag{3}$$

can be calculated numerically. The symbols U and W will be used to denote the horizontal and the vertical N respectively.

The values of Q were taken from Gutenberg [6; see his table 5c].

For the angles of incidence encountered in this work (0° − 40°) the values of F_n for the waves crossing the discontinuities separating the crustal layers are very close to unity. For this reason the effects of these discontinuities on all types of waves under consideration were neglected, and only F due to the reflection at the mantle-core boundary was used. These values were taken from Dana [2, 3].

For the absorption factor, $k = 0.00012$/km. was used and the distance was read approximately from an actual plot of the ray path.

For the direct P and S waves, i_0 was computed as a function of the epicentral distance Δ from Benndorf's theorem:

$$\sin i_0 = \frac{V_0}{\bar{v}_\Delta}, \tag{4}$$

where V_0 is the wave velocity at the surface of the earth and $\bar{v}_\Delta$ is the apparent velocity at the epicentral distance Δ. Gutenberg's recent figures for V_0, namely, $V_0(S) = 3.6$ km/sec. and $V_0(P) = 6.5$ km/sec., were used.

Again, for the direct P and S waves, i_h was computed from the formula

$$\frac{r \sin i}{v} = \text{const.}, \quad \text{(along the same ray)} \tag{5}$$

assuming the following velocities at different depths:

h (km.)	V_h (P) (km/sec.)	V_h (S) (km/sec.)
0	6.5	3.6
100	8.0	4.5
400	9.2	5.1
700	10.6	5.9

For PcP, PcS, ScS, ScP waves, i_0 and i_h and Δ were calculated as a function of the angle of incidence at the mantle side of the mantle-core boundary (i_c); i_0 and Δ were taken from Dana [2], corresponding to a given i_c, and Δ's were then corrected for the depth of focus (these corrections for P and S waves were given in Gutenberg and Richter [11, first paper; see their tables 1*a* and 3*a* respectively]; i_h was computed from formula (5), making the following assumptions:

r_c = the radius of the core = 3,466 km.

V_c = the velocity in the mantle just outside the core, $V_c(P) = 13.7$ km/sec., $V_c(S) = 7.25$ km/sec.

After i_0 and i_h are determined as described above, cos i_h is plotted against Δ. By measuring the slope of this curve, (d cos $i_h/d\Delta$) can be obtained. This is the only quantity involved in the calculation that does not vary smoothly, if $\bar{V}_\Delta$ values are used to calculate i_0 and i_h. For the direct P and S waves, $\bar{V}_\Delta$ were determined for every five degrees of epicentral distance, using Pasadena travel-time curves and tables; then cos $i_h = f(\Delta)$ curves were plotted and smoothed and the slopes were measured. For PcP, PcS, ScS, and ScP waves, i_0, i_h, and Δ were calculated as a function of i_c.

The calculated values are given in tables 1–6 below as $A = 6.3 - \log U$ (or $6.3 - \log W$).

Observed Ground Displacements

Materials used for this research were obtained from the seismograms recorded at Pasadena. Most of the intermediate and deep-focus shocks were recorded in the years 1940–1945. Some well-recorded shocks from 1937 to 1940 and a few shocks later than 1945 were also included. After combining N–S and E–W components into one horizontal component vectorially, the percentage of readings for each instrument is as follows:

Long-period torsion horizontal, 36 per cent of the total horizontal readings
Long-period Benioff horizontal, 48 per cent of the total horizontal readings
Short-period Benioff horizontal, 16 per cent of the total horizontal readings
Long-period Benioff vertical, 50 per cent of the total vertical readings
Short-period Benioff vertical, 50 per cent of the total vertical readings

The magnification curves were taken from Martner [14]. He discusses the determination of the dynamic magnification of the electromagnetic seismographs in detail. It is sufficient to repeat here that the relative amplifications (the response characteristics) of these seismographs are more accurately known than their absolute magnifications, so that the ratios of the amplitudes of two different waves (e.g., PcP/P) read on the same seismogram are more accurate than the individual ones.

In order to compare the observed values with the calculated ones, for each wave the largest amplitude recorded on a given seismogram is measured to the tenth of a millimeter and expressed in mm., and the period associated with this largest amplitude is read in seconds. Then the trace amplitude is multiplied by the factor $\frac{A_e/A^*}{T_e}$ (taken from Martner), where A_e is the amplitude of the ground motion in microns, A^* is the trace amplitude in millimeters, and T_e is the period of the ground motion, to get the A_e/T_e ratio, which is another symbol for $\frac{u, w}{T}$.

The average ratios of periods of the reflected waves to that of incident wave are shown below:

	T_{PcP}/T_P	T_{PcS}/T_P	T_{ScS}/T_S	T_{ScP}/T_S
Long-period instrument.....	0.92 (121)	1.46 (29)	0.85 (122)	0.80 (51)
Short-period instrument.....	0.93 (75)	1.15 (9)	1.0 (4)	.....

(Number of readings are shown in parentheses)

The accurate recognition of the various waves is the most important part of the problem.

The smallest distances encountered are those of Mexican intermediate shocks which start at $\Delta = 21\frac{1}{2}°$, and the largest Δ's belong to some Tonga–New Hebrides deep-focus earthquakes ranging up to $\Delta = 87\frac{1}{2}°$. A total of 631 readings for 69 shocks were used for this report. Their epicentral distances cover the range $21\frac{1}{2}°$–$87\frac{1}{2}°$. The focal depth varies from 70 km. to 650 km. Only twelve real deep-focus shocks ($h \geqq 300$ km.) are included in this work.

Methods of Comparing the Calculated and the Observed Ground Displacements

One method of comparison is to take the observed ratio of $\frac{u, w}{T}$ of the reflected wave to that of the incident wave and compare these with the ratio of N (formula 4) of the reflected wave to N of the incident wave. Since it is assumed that $K\sqrt{E_1}$ has the same value for all waves leaving the source as the same type, by taking the ratio of calculated N's (or U's and W's) for PcP/P, PcS/P, ScS/S, ScP/S the values of $K\sqrt{E_1}$ cancel in each case and the calculated ratios can be compared directly with the observed ratios.

The second method for comparing the calculated and the observed values consists of calculating the "A" values.

"A" values were defined by Gutenberg (7) as follows:

Theoretical A: $A_t = C - \log U$ (or $C - \log W$) (6)

Observed A: $A_0 = M - \log \left(\frac{u, \text{ or } w}{T}\right)_{obs.} - 0.1\,(M - 7) - 0.2$ (7)

where C is a constant which for practical purposes was assumed by Gutenberg to be 6.3 in all shocks for P waves and also for S waves (SV and SH combined) (Gutenberg [7]). For Pasadena, a station correction -0.2 was used in this work: last term in (7) above.

In formula (7), M is the magnitude of the earthquake in question as defined originally by Richter [16]. The magnitudes are determined (Richter [16], Guten-

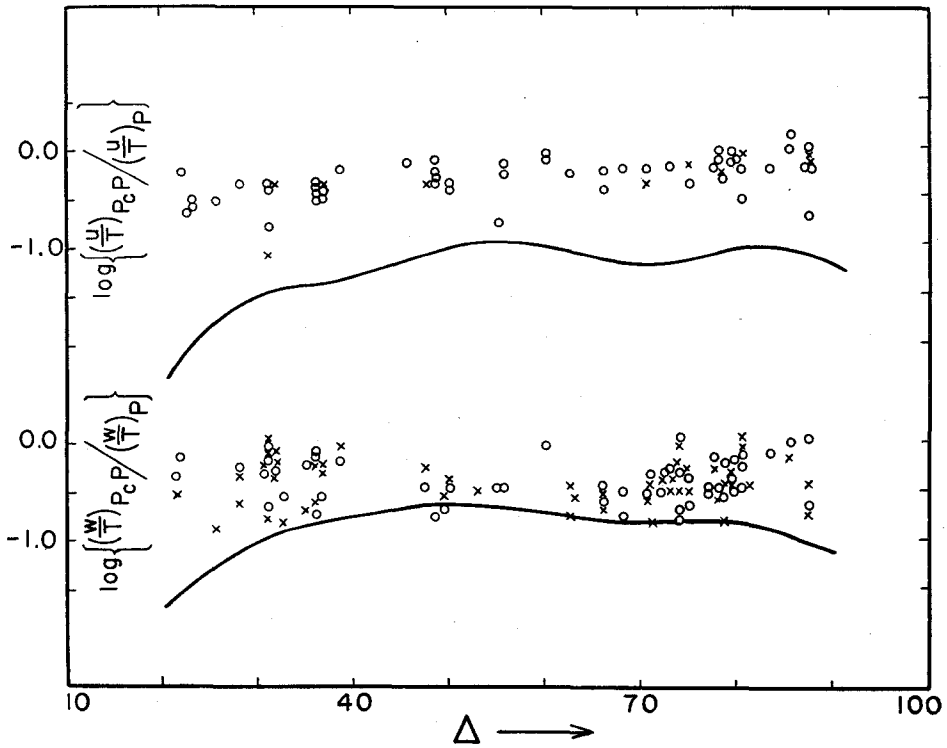

Fig. 1.

berg [7 and 8]) from observed amplitudes and periods, using a variety of stations, instruments, wave types (chiefly P, PP, and S), and distances.

For each observation, $A_t - A_o$, which we shall call "residual" in the following discussion, was determined. These residuals are plotted against the epicentral distance in figures 5–10. A positive residual ($A_t - A > 0$) means that the observed displacement/period is larger than the theoretical ones, and conversely.

RESULTS

In figure 1, $\log\left\{\left(\frac{u, w}{T}\right)_{PcP}/\left(\frac{u, w}{T}\right)_{P}\right\}$ is plotted against the epicentral distance. The solid curves are the corresponding theoretical ratios. The average discrepancy (observed minus computed) between the observed and the theoretical ratios of the horizontal component is about $+0.8$,[3] except for $\Delta < 30°$, where it is still higher. It is important to note here that no definite appreciable effect of the epicentral dis-

[3] These figures are the logarithms of the quantities involved.

tance on the discrepancy can be detected from the results. For the vertical component of the same ratio, observed values are on the average higher than the theoretical ones, but not as much as in the case of the horizontal component, the average discrepancy being approximately +0.3 or +0.4. For epicentral distances between 40° and 60° the agreement is fairly good. In any case, when an explanation for the abnormal discrepancies observed is sought, the horizontal component ratios are the ones

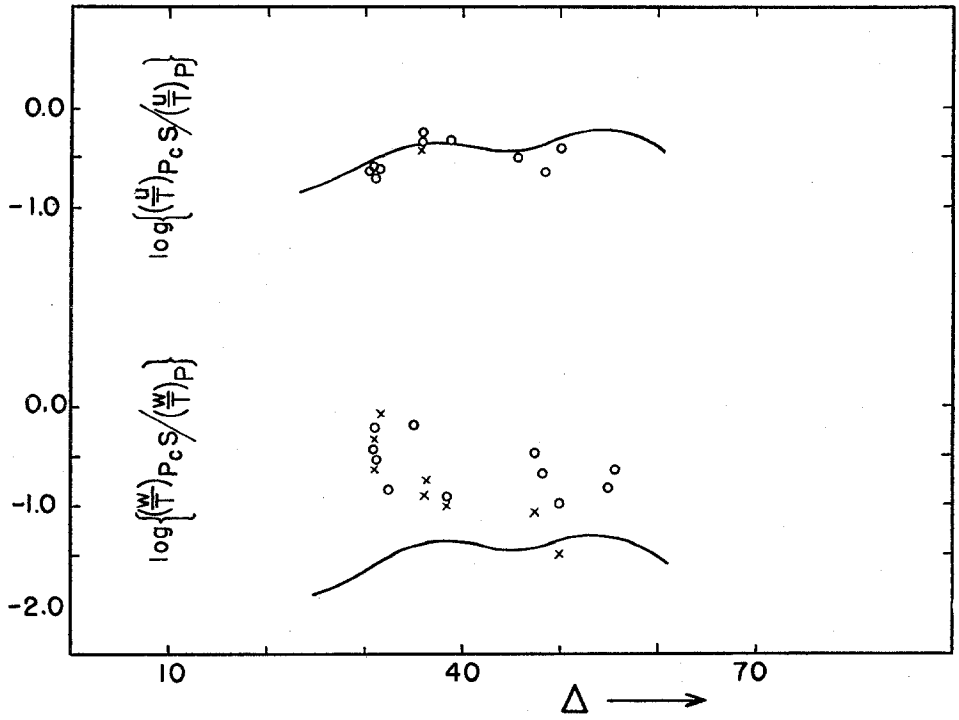

Fig. 2.

that should attract more attention, although any explanation that can be proposed should not change the vertical component ratios in the wrong direction.

The data for ScP/S (fig. 2) are not abundant, and they only cover an epicentral range 25°–50°. However, the available data definitely show that the observed horizontal ratios are about five or more than five times larger than the theoretical ones around 30°–35°, decreasing somewhat as the epicentral distance becomes larger. The same effect of the epicentral distance can be observed for the vertical-component ratios; here, the average discrepancy is about +0.4, indicating that the observed ratios are about two or three times larger than the theoretical ones.

The horizontal component of the observed ratios of PcS/P (fig. 3) are in good agreement with the theoretical ratios. Although only a limited number of data are available, nevertheless all the points of the observed values fall along the calculated curve. As PcS arrive right after ScP and close to it, in many instances it is difficult to identify them separately. However, the difference in the arrival times of these two waves increases with the focal depth. Although the observed ratios for the hori-

zontal component of PCS/P fit the theory nicely, the observed vertical displacement ratios are on the average five times larger than the calculated ratios.

The observed horizontal ScS/S (fig. 4) ratios (SH/SV is assumed to be "one") are in fairly good accord with the theoretical results except for $\Delta < 40°$, where they are larger. The observed vertical component ratios of ScS/S are ten or more times larger than the corresponding theoretical values around $\Delta = 30°$. This difference

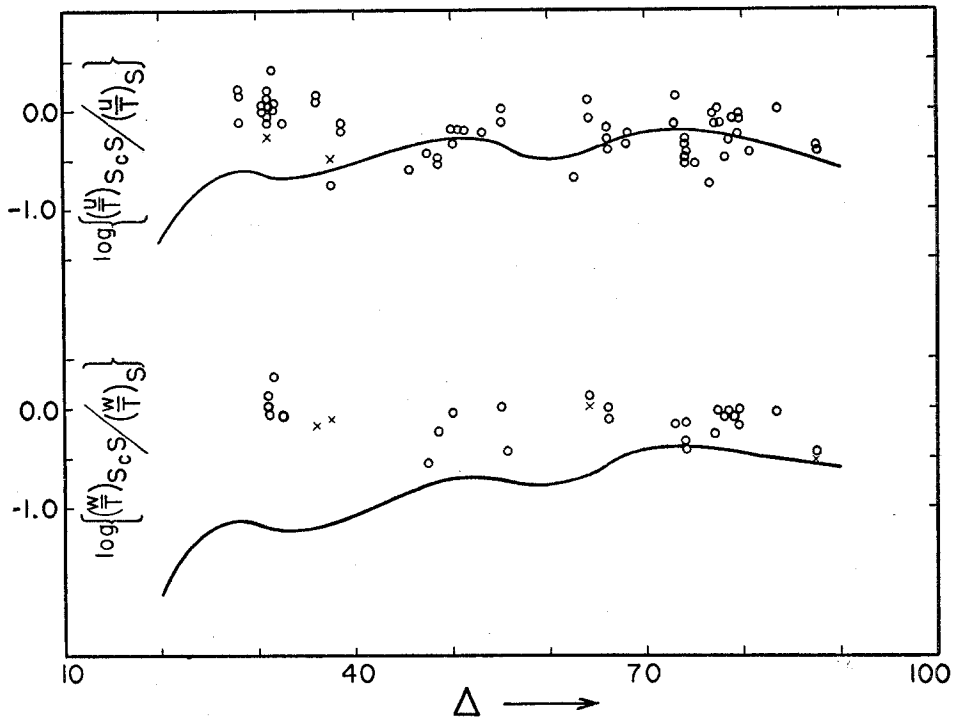

Fig. 3.

decreases as Δ increases, and for $\Delta = 70°$ the observed results fit the theoretical curve nicely.

The foregoing analysis of data can be summarized as follows. The observed ratios of the horizontal displacements of the waves that are reflected as P wave at the mantle-core boundary to those of the incident wave are on the average six or seven times larger than the theoretical ratios. The observed ratios of the vertical components of these waves are only two or three times larger than the theoretical ones. (This group includes PcP/P and ScP/S.) For the waves that are reflected as S wave at the same boundary, the observed horizontal-component ratios are in fairly good agreement with the theoretical ratios, but the observed vertical-component ratios of the same waves are considerably larger than the theoretical ones. (This group includes ScS/S and PcS/P.) The vertical-component ratios of ScS/S and PcS/P show some effect of the epicentral distance; the discrepancy between the theoretical

and the observed ratios decreases at large epicentral distances. These conclusions are presented in the following table in a more condensed form:

Observed ground displacement/period ratios: greater than the theoretical ratios		Observed ground displacement/period ratios: in fairly good agreement with the theoretical ratios	
Horizontal	Vertical	Horizontal	Vertical
PcP/P	PcS/P	PcS/P	PcP/P
ScP/S	ScS/S	ScS/S	ScP/S

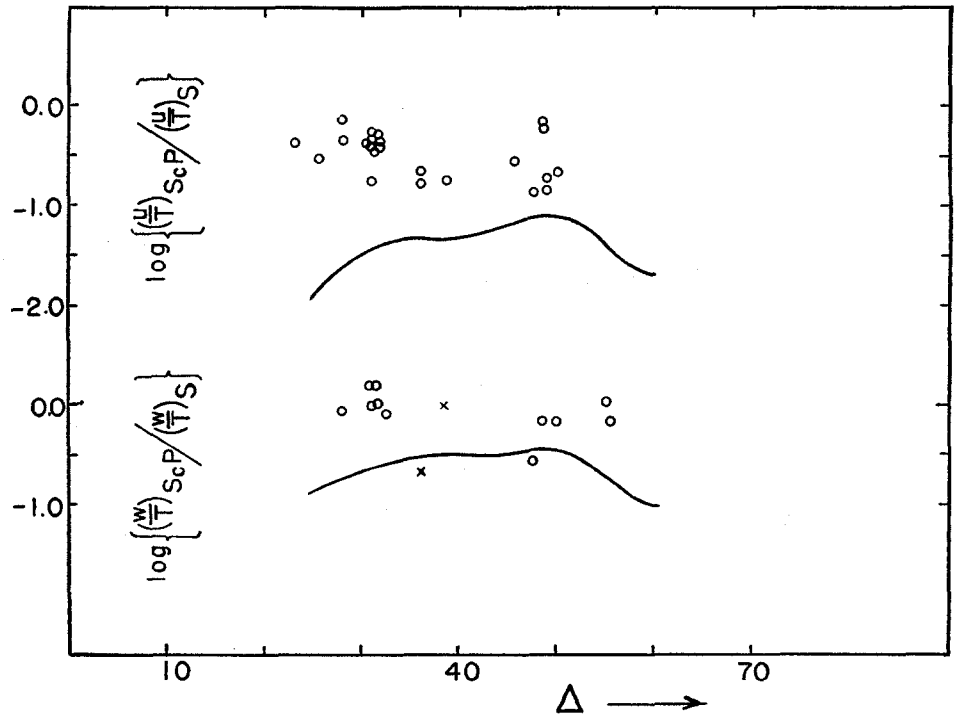

Fig. 4.

The results obtained from $A_t - A_o$ residuals as a function of the focal depth are in good agreement with those that were obtained from the study of the ground displacement/period ratios. The depth of focus does not play any role in the variation of the residuals.

The average residuals are tabulated below.

	Average residual	
	Horizontal component	Vertical component
P	±0.*	±0.0
PcP	+0.8	+0.4
PcS	±0.0	+0.6
S	−0.1	−0.1
ScS	+0.1	+0.5
ScP	+0.75	+0.35

* These figures are the logarithms of the quantities involved.

The residuals $A_t - A_o$ are plotted against the epicentral distance in figures 5–10. Here again each figure consists of two parts, the upper part representing the horizontal component and the lower the vertical component. The characteristic features of the residuals as a function of the epicentral distances are listed below.

1. Direct P wave (fig. 5)

a. Horizontal component: The mean residual curve can be represented by a straight line that has a slight positive slope. The residual is negative for $\Delta < 35°$,

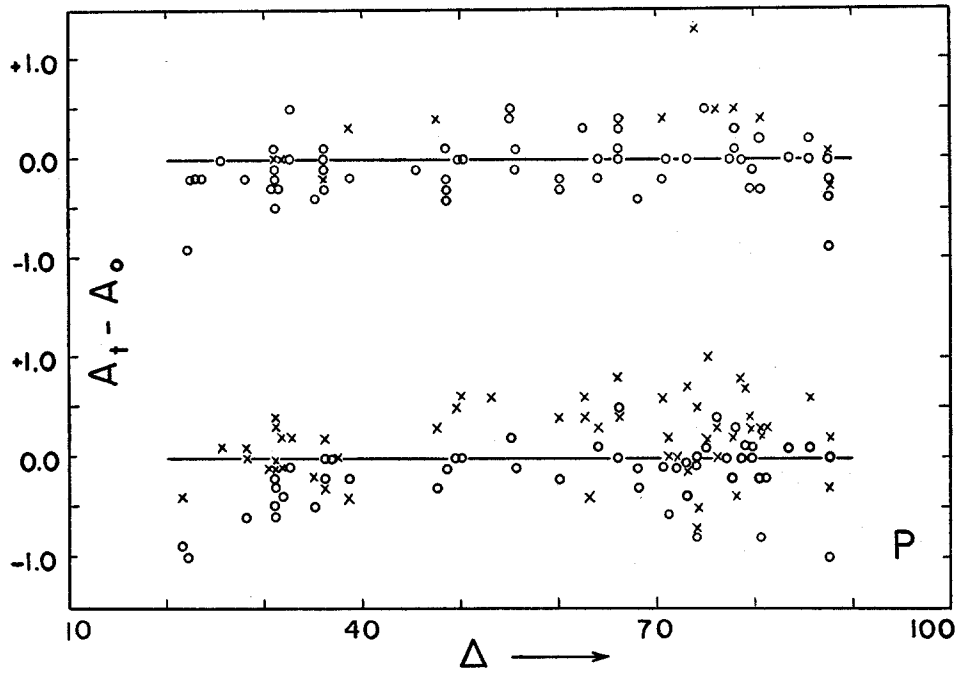

Fig. 5.

and positive for $\Delta > 35°$, thus increasing slightly with the increasing epicentral distance. However, this mean residual line is very close to the zero line at all distances.

b. Vertical component: These residuals as a whole have a picture similar to that of the horizontal-component residuals.

2. PcP (fig. 6)

a. Horizontal component: For all epicentral distances a line parallel to the zero line can be drawn to represent a mean residual which is approximately +0.8. The residuals for $\Delta < 30°$ are somewhat higher than this over-all mean.

b. Vertical component: The line representing the mean residuals has a very slight positive slope. The over-all mean residual is about +0.3 (putting more weight on the readings from the long-period seismograph seismometers).

3. PcS (fig. 7)

a. Horizontal component: There are only a few readings for this wave, all of which line up around the zero line so that the over-all average residual is ±0.

b. Vertical component: The over-all mean residual is approximately +0.7.

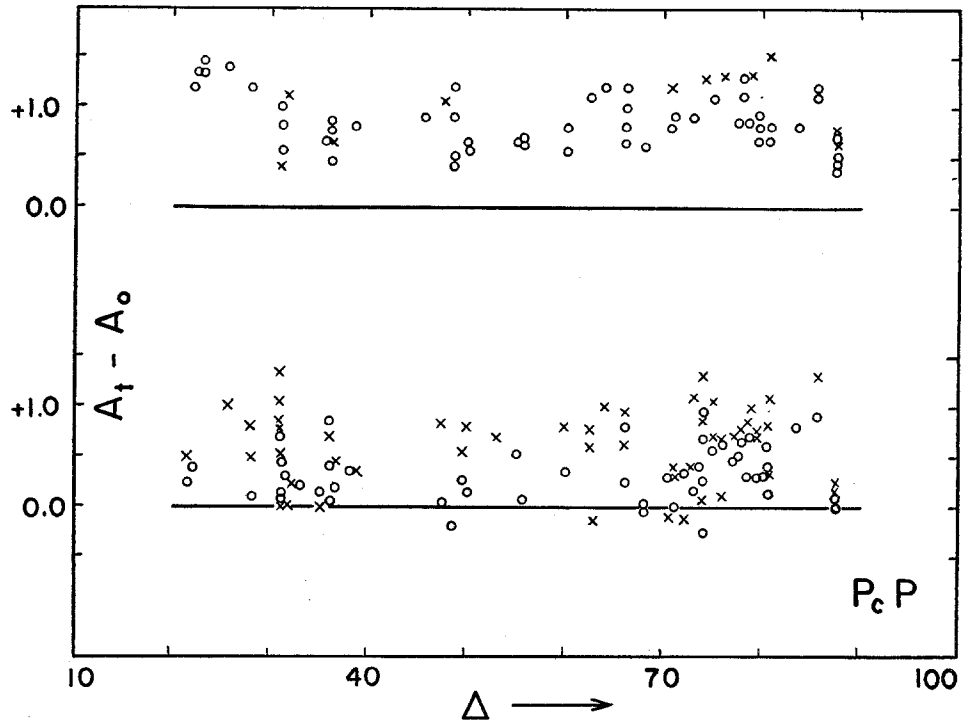

Fig. 6.

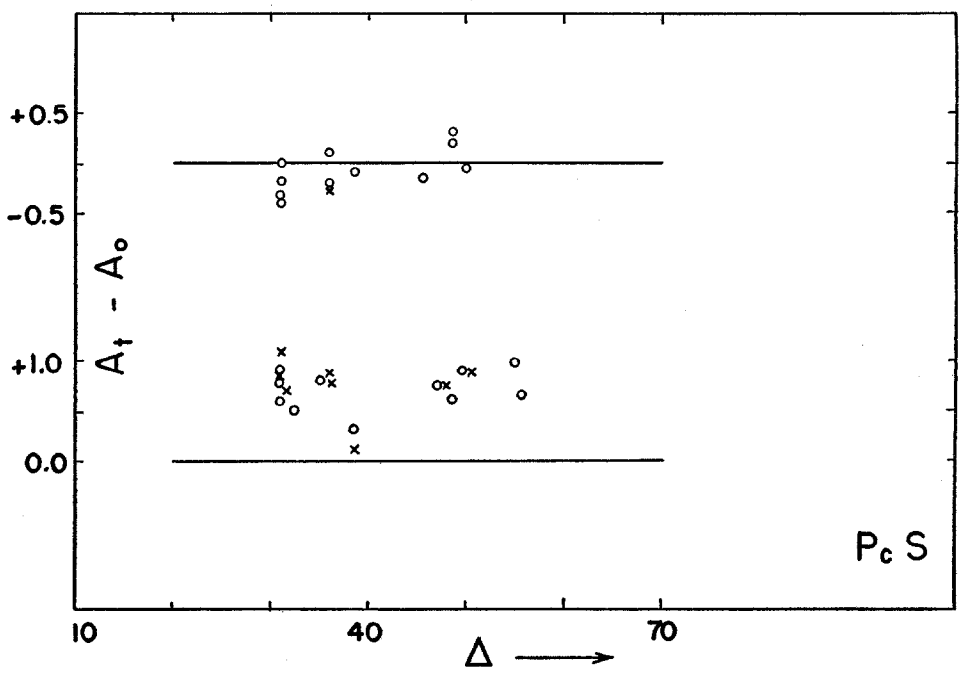

Fig. 7.

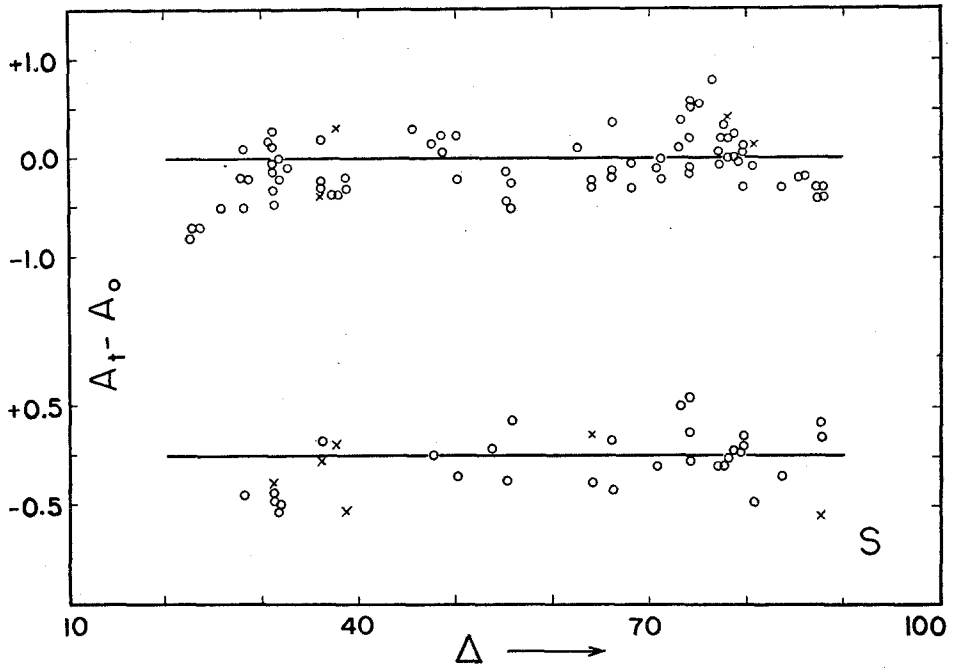
+1.0
0.0
-1.0
+0.5
-0.5
$A_t - A_o$
S
10
40
70
100
Δ

Fig. 8.

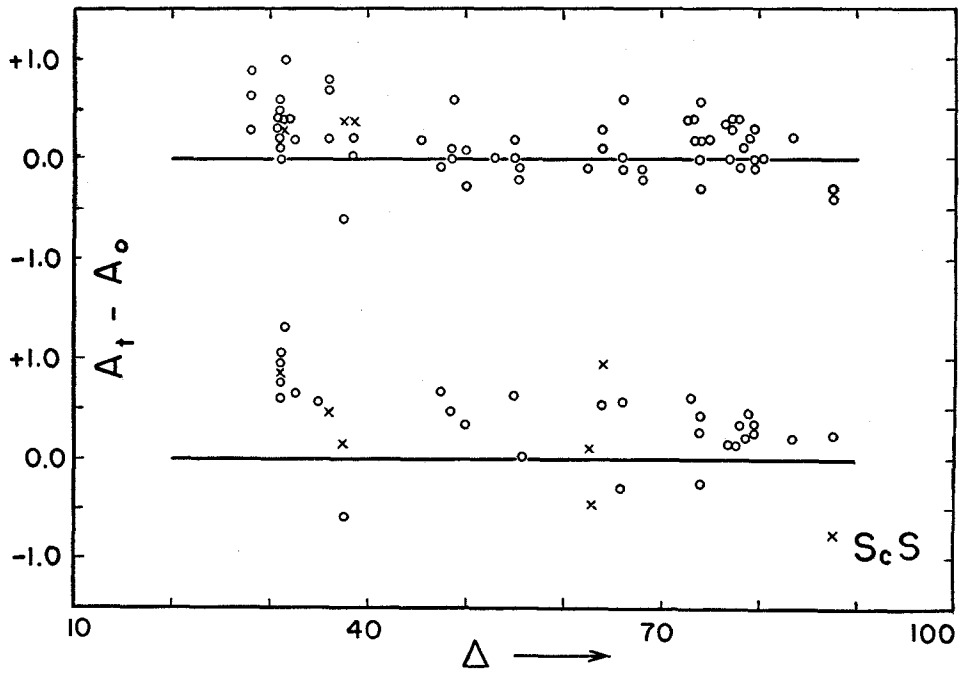
+1.0
0.0
-1.0
+1.0
0.0
-1.0
$A_t - A_o$
ScS
10
40
70
100
Δ

Fig. 9.

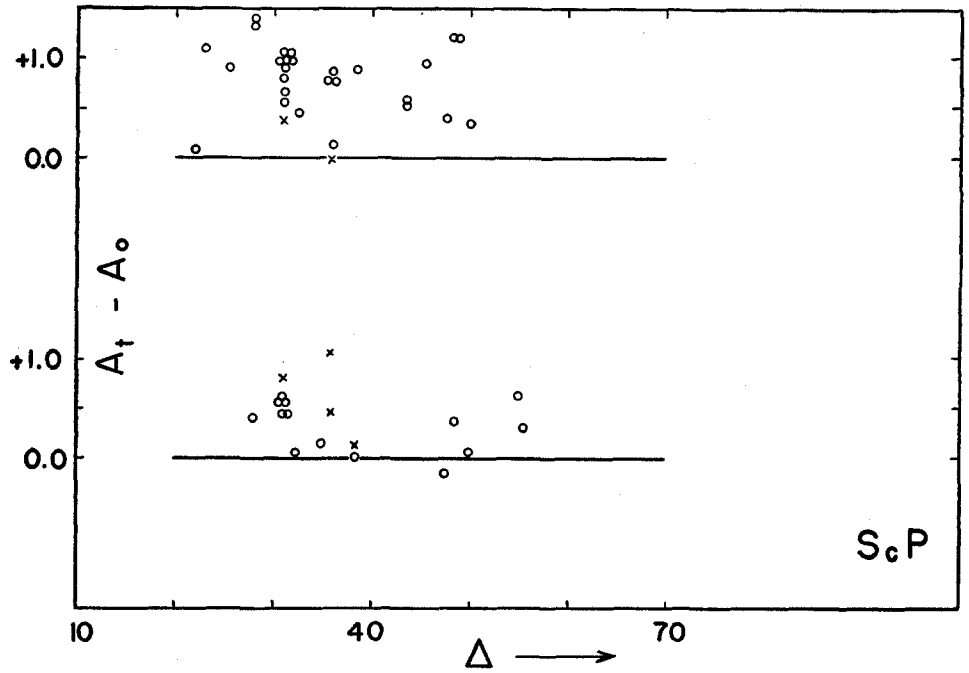

Fig. 10.

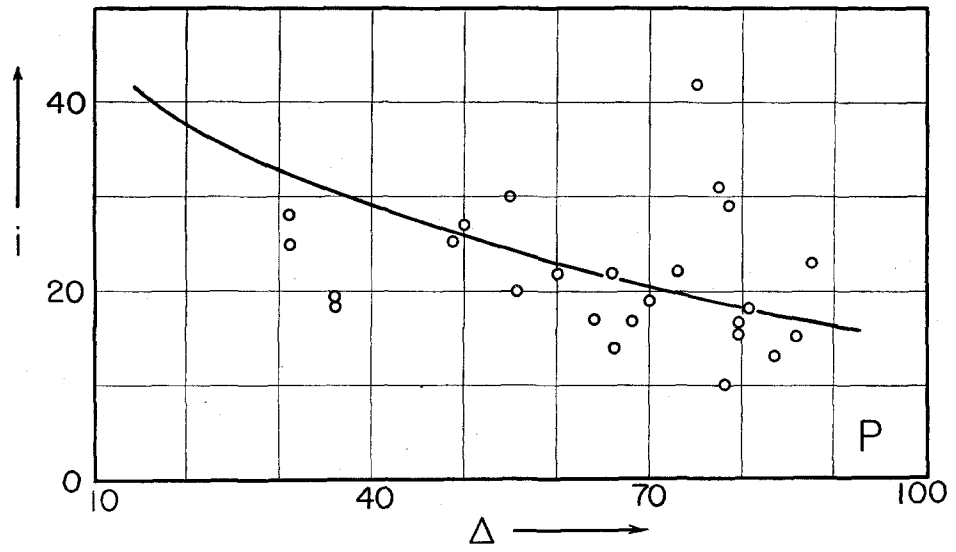

Fig. 11.

4. S (fig. 8)

Both horizontal and vertical components have an average residual line with a slight positive slope. The over-all mean value is slightly negative for both.

5. ScS (fig. 9)

a. Horizontal component: The line representing the average residuals has a slight negative slope. Over-all mean is very close to zero.

b. Vertical component: Here again we observe a very slight negative slope. The over-all mean residual is about +0.3. The residuals for $\Delta < 40°$ are considerably larger than this over-all mean.

6. ScP (fig. 10)

a. Horizontal component: Here too a slight negative slope is present. The over-all mean residual is approximately +0.75.

b. Vertical component: The mean residual line is parallel to the zero line and the over-all mean is about + 0.3.

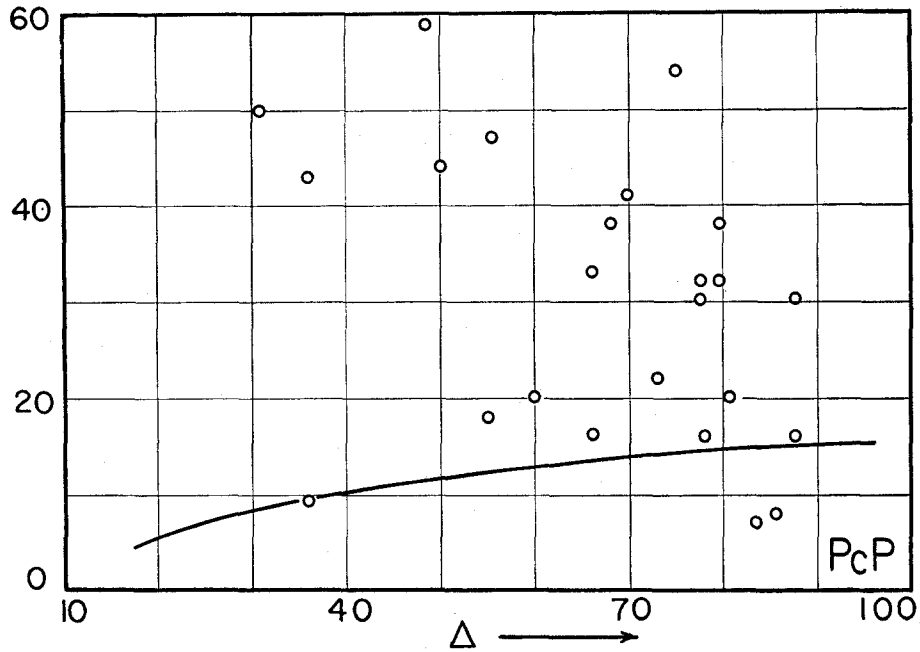

Fig. 12.

The foregoing analysis of the characteristic features of the residuals as a function of the epicentral distance show that the results are again in good agreement with those that were obtained by considering the displacement ratios which were summarized on page 70.

The advantage of the residual $(A_t - A_o)$ method is that it brings up the individual features of the displacements for each wave separately.

OBSERVED APPARENT ANGLES OF INCIDENCE

The large observed horizontal-component ratios of PcP/P and other anomalous large observed results have led us to investigate the observed angles of vibration for P, PcP, S, and ScS waves. The observed angle of vibration $\bar{\imath}$ is calculated by

$$\bar{\imath} = \tan^{-1}\left(\frac{u}{w}\right)_{\text{obs.}} \quad \text{(for longitudinal waves)}.$$

To calculate $\bar{\imath}$ by this formula we used u and w as obtained from the same type of horizontal and vertical instruments. For this purpose only long-period Benioff in-

struments supplied sufficient data. The results are shown in figures 11 and 12 for P and PcP waves respectively. The observed angle of vibration of PcP has an average value 35°–40°. There is a tendency for the observed $\bar{\imath}$ to decrease slightly as Δ increases. The angle of incidence (i_0) of PcP as calculated from the apparent velocity of PcP by Benndorf's theorem starts from zero at $\Delta = 0$, increases slowly as the epicentral distance increases, and reaches a value little more than 15° at the largest epicentral distances. The observed angles of vibration of the P wave are somewhat smaller than the theoretical angles of incidence at small epicentral distances, and larger for large epicentral distances; but in general they fit the present theory fairly well.

From the consideration of the angles of vibration of the direct P wave and PcP wave it can be concluded that the anomalous character of the observed ground displacement/period ratios of PcP/P are due to the behavior of the PcP wave and not due to the behavior of the P wave. This fact is further evidenced by the results of $A_t - A_0$ residuals.

The angles of vibration of S-type waves can be obtained from the formula

$$\bar{\imath} = \tan^{-1}\left(\frac{w}{u}\right)_{\text{obs.}}$$

Using ground displacement values that were obtained from the records of the long-period horizontal-component and vertical-component Benioff electromagnetic instruments, $\bar{\imath}$'s for S and ScS were determined. These angles of vibration are plotted in figures 13 and 14 respectively. On the average, the observed angle of vibration for ScS is about 32° at all epicentral distances, which is considerably larger than the calculated angles of incidence. On the other hand, the average observed angle of vibration for the direct S wave is somewhat smaller than the calculated angle of incidence at small epicentral distances, and larger at large epicentral distances; but in general they are fairly close to the theoretical angles of incidence. This result, as should be expected, is in accord with the result mentioned previously that the observed and calculated ground displacement/period ratios of ScS/S are in better agreement at large epicentral distances.

According to the present theory, the angle of vibration ($\bar{\imath}$) of both P and S waves should differ from the angle of incidence (i_0), for the range of values considered here, by only about 2°–3° at the most, assuming of course that for longitudinal waves the vibration is in the direction of propagation, and that for transverse waves the vibration is perpendicular to the direction of propagation. The observational results strongly indicate that for PcP the vibration is not in the direction of propagation, and that for ScS the vibration is not perpendicular to the direction of propagation.

The angle between the normal and the direction of the ground vibration produced upon the incidence of a PcP wave at the surface of the earth is shown in figure 15.

In order to check the angle of incidence (angle of arrival) of the PcP wave, nine Mexican and Central American shocks were selected which were recorded at all three stations, namely, Pasadena, Palomar, and Tinemaha. The differences of arrival times (d) of PcP between two stations that line up with the epicenter were

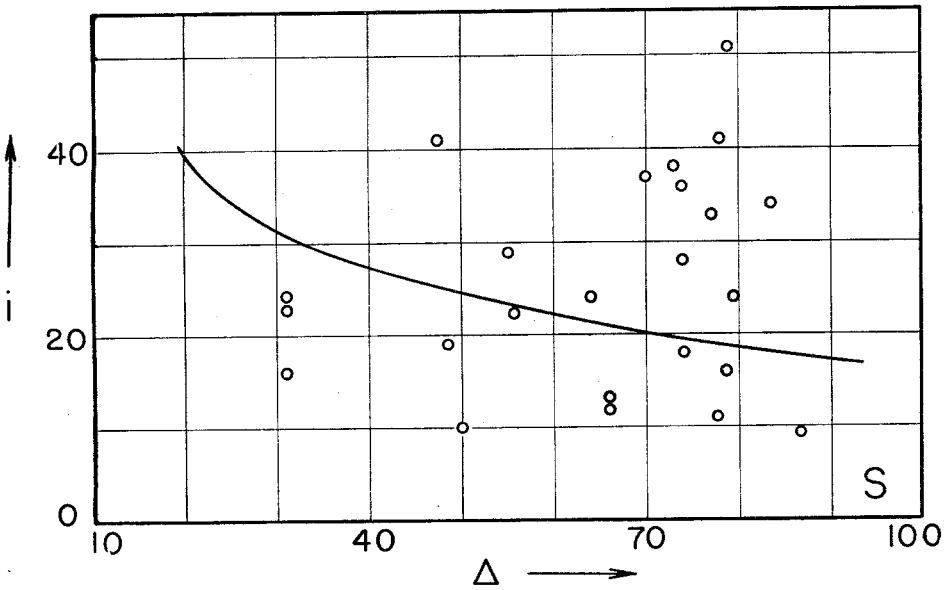

Fig. 13.

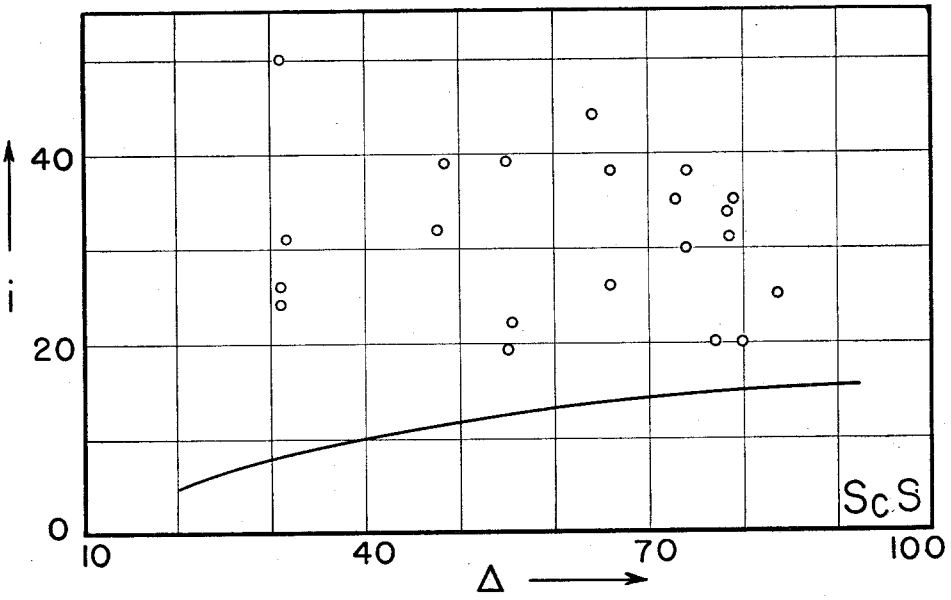

Fig. 14.

obtained from the Bulletins of the Seismological Laboratory at Pasadena, and are listed below:

Out of nine cases (Pasadena–Palomar):	for 2 shocks, d = 2 seconds
	for 4 shocks, d = 3 seconds
	for 2 shocks, d = 4 seconds
	for 1 shock , d = 7 (?) seconds
Out of eight cases (Tinemaha–Palomar):	for 4 shocks, d = 8 seconds
	for 3 shocks, d = 9 seconds
	for 1 shock , d = 14 (?) seconds

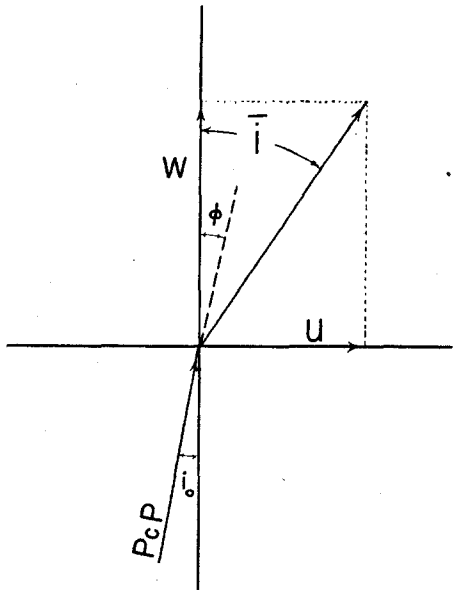

Fig. 15.

In both cases, except only for one shock, these differences are in close agreement with the ones given by the travel-time curves for the corresponding focal depth and the epicentral distance range (31°–35°).

Discussion of the Results, and Conclusion

In the last section, the facts that could be detected from the data were presented without any attempt at explanation. It is now possible to discuss them and to seek explanations of the observed results.

The fact that the same results were obtained by another investigator minimizes, if it does not eliminate, systematic error of measurements as the cause of the discrepancies. As was mentioned earlier, the instrumental constants are fairly accurate; and if the displacement ratios instead of individual displacements are considered, the accuracy is higher. Hence the sources of error must be sought in the assumptions involved in the derivation of the theoretical equations (1) and (2). Martner [14] has carefully reconsidered each factor involved in equation (2), making alternate possible assumptions regarding the velocities of the P wave near the surface of the

earth, in the mantle just outside the core, and in the core near the mantle-core boundary. He has also tried alternate possible density ratios at the mantle-core boundary. The effects of these alternate assumptions as calculated by Martner can be summarized as follows.

To calculate the energy ratios of the reflected and the refracted waves at the mantle-core boundary, Dana [3] had used the following velocities and densities: V (P, mantle) = 13.7 km/sec., V (P, core) = 8.0 km/sec., ρ (core/ρ (mantle) = 10.1/5.4. Leaving V (P, mantle) as 13.7 km/sec. and assuming for V (P, core) = 7 km/sec. and 9 km/sec. and for $\rho_2/\rho_1 = 2.0$, 1.5, and 1.0, Martner calculated different curves for $\sqrt{E_{\text{reflected P}}/E_{\text{incident P}}}$ for six possible combinations of these parameters. He finds that only when V (P, core) = 9 km/sec. and $\rho_2/\rho_1 = 2.0$ is the energy ratio curve above the curve given by Dana, and in that case it only increases by 16 per cent. Assuming the longitudinal wave velocity near the surface of the earth to be 8.0 km/sec., Martner has calculated the theoretical angles of incidence for PcP. This higher velocity gives an angle of incidence at the largest epicentral distance of about 18½°, which is only three degrees larger than the one we have obtained on the assumption that the longitudinal velocity near the surface is 6.5 km/sec., and still far smaller than the observed apparent angle of incidence.

The observed large ground displacements due to PcP and others may seem to suggest that the energy released at the focus does not propagate equally in all directions. This would mean that a larger fraction of energy is propagated vertically downward (thus going into PcP wave) and decreasing as the angle of incidence at the focus increases. If this were the case, the energy going into P and PcP waves at large epicentral distances should be nearly the same and the observed values should fit the theoretical curve at the large epicentral distances; and, too, the discrepancies for the horizontal and the vertical components should be the same. But the results are far different: the discrepancies for PcP/P ratio are almost the same for all distances.

Thus, we are unable to explain the large observed ground displacements due to the waves that are reflected at the mantle-core boundary by any alternate possible assumptions in regard to the velocity and the density distribution in the neighborhood of the discontinuity, and the velocity near the surface of the earth. The azimuths as calculated from PcP show no appreciable departure from those that are calculated from P, and the angle of arrival as calculated from the arrival-time differences of PcP between two near-by stations which line up the epicenter show no departure from the present theory of propagation of the seismic waves. But we have strong evidence that the ground vibrations due to PcP waves are not in the direction of propagation at the recording station, whereas the vibration due to the direct longitudinal wave is nearly in the direction of propagation. It seems logical that at this point we ask: "Is it possible to have a P wave for which the vibration is not in the direction of propagation? Could it be a combination of transverse and longitudinal waves traveling together?" The theory shows that in an isotropic medium soon after reflection longitudinal and transverse waves will separate as they travel with different velocities. As early as 1911 Rudzki [17] investigated the propagation of a disturbance in an anisotropic medium. He considered the case of the crustal layers of the earth and assumed the medium to be transversely isotropic and

vertically anisotropic. Recently, Stoneley [18] published a paper in which he considers the same problem in the same manner. Rudzki's original paper, in which reflection and refraction under assumed conditions were also considered, was not available to the present writer. In a review of Rudzki's paper it is indicated that under these conditions there will neither be a purely longitudinal nor a purely transverse wave. Stoneley expresses the same opinion in the following words: "Under these assumptions, with body waves the sharp distinction into compressional and distortional waves does not hold." Stoneley does not go into the problem of reflection and refraction; he merely indicates that by setting up the relevant boundary conditions the reflection and refraction can be worked out.

Further theoretical research is needed to solve the problem.

Note added in proof.—After this paper was sent to the publisher, this problem was studied by a different method of approach, which gave some light on the cause of the discrepancies found. See Kazim Ergin, "Observations on the Recorded Ground Motion Due to P, PcP, S, ScS," *Bull. Seism. Soc. Am.*, 43:263–270 (1952).

TABLE 1

VALUES OF $A = 6.3 - \log U$ (or $6.3 - \log W$) AS A FUNCTION OF Δ (IN DEGREES), FOR P

Δ	h = 100 km. Horizontal	h = 100 km. Vertical	h = 400 km. Horizontal	h = 400 km. Vertical	h = 700 km. Horizontal	h = 700 km. Vertical
20	5.8	5.6	5.8	5.7		
25	6.1	6.0	6.2	6.0	6.2	6.0
30	6.3	6.2	6.5	6.3	6.4	6.2
35	6.6	6.4	6.6	6.4	6.3	6.1
40	6.6	6.4	6.4	6.3	6.3	6.0
45	6.6	6.4	6.5	6.3	6.6	6.3
50	6.8	6.6	6.7	6.4	6.8	6.6
55	7.0	6.7	6.6	6.4	6.6	6.4
60	6.9	6.6	6.7	7.4	6.6	6.3
65	6.8	6.5	6.8	6.5	6.7	6.4
70	6.8	6.5	6.8	6.5	6.7	6.4
75	7.0	6.6	7.0	6.6	7.0	6.4
80	7.1	6.8	7.1	6.7	6.9	6.5
85	7.2	6.8	7.2	6.8	7.0	6.6
90	7.2	6.7	7.1	6.7	7.2	6.7
95	7.6	7.0	7.2	6.7	7.3	6.8
100	7.4	7.0	7.5	7.0	7.4	6.9

TABLE 2

VALUES OF $A = 6.3 - \log U$ (OR $6.3 - \log W$) AS A FUNCTION OF Δ (IN DEGREES), FOR PcP

Δ	h = 100 km. Horiz.	h = 100 km. Vert.	Δ	h = 400 km. Horiz.	h = 400 km. Vert.	Δ	h = 700 km. Horiz.	h = 700 km. Vert.
8.1	9.0	7.7	8.0	8.9	7.6	7.9	8.9	7.6
16.7	8.5	7.5	16.4	8.4	7.4	16.0	8.3	7.3
25.3	8.1	7.3	24.8	8.0	7.2	24.1	7.9	7.0
34.4	7.9	7.2	33.8	7.8	7.1	32.8	7.7	7.0
44.8	7.8	7.2	44.0	7.7	7.1	42.8	7.6	7.0
56.4	7.7	7.2	55.5	7.7	7.1	54.2	7.6	7.0
71.2	8.0	7.4	70.3	7.9	7.3	68.8	7.8	7.3
91.3	8.4	7.8	90.3	8.3	7.8	88.8	8.2	7.7
97.8	9.5	9.0	96.8	9.5	9.0	95.3	9.5	8.9
102.8	7.9	7.4	101.8	7.8	7.3	100.3	7.8	7.3

TABLE 3

VALUES OF $A = 6.3 - \log U$ (OR $6.3 - \log W$) AS A FUNCTION OF Δ (IN DEGREES), FOR PcS

Δ	h = 100 km. Horiz.	h = 100 km. Vert.	Δ	h = 400 km. Horiz.	h = 400 km. Vert.	Δ	h = 700 km. Horiz.	h = 700 km. Vert.
0.0	∞	∞	0.0	∞	∞	0.0	∞	∞
6.3	7.4	9.0	6.2	7.3	8.9	6.1	7.2	8.8
12.6	7.1	8.4	12.3	7.9	8.3	12.0	6.9	7.9
19.0	7.0	8.1	18.5	6.9	8.0	17.8	6.8	7.9
25.6	6.9	7.9	25.0	6.8	7.8	24.1	6.8	7.7
32.9	7.0	7.9	32.1	6.9	7.8	30.9	6.8	7.7
40.2	7.1	7.9	39.3	7.0	7.8	38.0	6.8	7.7
48.6	7.2	8.0	47.7	7.0	7.8	46.2	7.0	7.8
57.5	7.3	8.1	56.6	7.2	8.0	55.5	7.1	7.9
61.2	7.4	8.2	60.2	7.3	8.1	58.7	7.2	8.2
65.0	∞	∞	64.0	∞	∞	62.5	∞	∞

TABLE 4

VALUES OF $A = 6.3 - \log U$ (OR $6.3 - \log W$) AS A FUNCTION OF Δ (IN DEGREES), FOR SV

Δ	h = 100 km. Horiz.	h = 100 km. Vert.	h = 400 km. Horiz.	h = 400 km. Vert.	h = 700 km. Horiz.	h = 700 km. Vert.
20	6.5	5.7	...	...	...	...
25	5.8	6.1	5.8	6.0	5.9	6.1
30	6.2	6.4	6.1	6.3	6.2	6.5
35	6.4	6.6	6.3	6.5	6.3	6.5
40	6.4	6.6	6.3	6.6	6.2	6.5
45	6.5	6.8	6.4	6.6	6.4	6.6
50	6.8	7.0	6.5	6.8	6.4	6.7
55	6.5	6.8	6.5	6.8	6.3	6.6
60	6.5	6.8	6.4	6.7	6.3	6.6
65	6.6	6.9	6.6	6.9	6.5	6.8
70	6.7	7.1	6.8	7.1	6.7	7.1
75	7.0	7.3	6.8	7.1	6.6	6.9
80	6.9	7.2	6.7	7.0	6.5	6.9
85	6.6	7.0	6.6	6.9	6.5	6.8
90	6.6	7.1	6.5	7.0	6.5	7.0
95	6.8	7.3	6.8	7.2	6.8	7.2
100	7.0	7.4	7.0	7.5	6.9	7.4

TABLE 5

VALUES OF $A = 6.3 - \log U$ (OR $6.3 - \log W$) AS A FUNCTION OF Δ (IN DEGREES), FOR ScS

Δ	h = 100 km. Horiz.	h = 100 km. Vert.	Δ	h = 400 km. Horiz.	h = 400 km. Vert.	Δ	h = 700 km. Horiz.	h = 700 km. Vert.
8.2	6.6	7.8	8.0	6.5	7.8	7.7	6.4	7.7
17.2	6.7	7.6	16.8	6.6	7.6	16.3	6.5	7.4
26.1	6.8	7.6	25.5	6.7	7.5	24.8	6.6	7.4
26.9	6.8	7.6	26.3	6.7	7.5	25.6	6.6	7.4
27.9	6.6	7.4	27.3	6.5	7.3	26.5	6.4	7.2
30.5	7.0	7.7	29.8	6.9	7.7	29.0	6.8	7.6
35.5	7.1	7.8	34.8	7.0	7.7	33.8	6.9	7.6
46.1	7.1	7.7	45.3	7.0	7.6	44.2	7.0	7.6
58.1	7.0	7.6	57.1	7.0	7.5	55.9	6.9	7.4
72.4	7.0	7.5	71.4	6.9	7.5	69.9	6.8	7.4
90.8	7.2	7.7	89.7	7.2	7.6	88.1	7.0	7.5
100.8	7.3	7.8	99.7	7.3	7.8	98.0	7.2	7.6

TABLE 6

VALUES OF $A = 6.3 - \log U$ (OR $6.3 - \log W$) AS A FUNCTION OF Δ (IN DEGREES), FOR ScP

Δ	h = 100 km. Horiz.	h = 100 km. Vert.	Δ	h = 400 km. Horiz.	h = 400 km. Vert.	Δ	h = 700 km. Horiz.	h = 700 km. Vert.
0.0	∞	∞	0.0	∞	∞	0.0	∞	∞
12.7	8.4	7.4	12.6	8.3	7.3	12.3	8.2	7.2
28.9	7.9	7.2	28.4	7.8	7.1	27.8	7.7	7.0
48.7	7.9	7.4	48.2	7.9	7.4	47.4	7.8	7.3
54.4	8.0	7.5	53.8	8.0	7.5	53.0	7.9	7.4
65.4	∞	∞	64.7	∞	∞	63.8	∞	∞

REFERENCES

1. Bullen, K. E., *An Introduction to the Theory of Seismology* (Cambridge University Press, 1947).
2. Dana, S. W., *Amplitudes of Seismic Waves Reflected and Refracted at the Earth's Core*, unpubl. diss., California Institute of Technology, Pasadena (1944).
3. Dana, S. W., "The Partition of Energy among Seismic Waves Reflected and Refracted at the Earth's Core," *Bull. Seism. Soc. Am.*, 34: 189–197 (1944).
4. Dana, S. W., "The Amplitudes of Seismic Waves Reflected and Refraced at the Earth's Core," *Bull. Seism. Soc. Am.*, 35: 27–35 (1945).
5. Gutenberg, B., "Theorie der Erdbebenwellen," *Handbuch der Geophys.*, Vol. 4, pp. 1–80 (1932).
6. Gutenberg, B., "Energy Ratio of Reflected and Refracted Seismic Waves," *Bull. Seism. Soc. Am.*, 34: 85–102 (1944).
7. Gutenberg, B., "Amplitudes of P, PP, and S and Magnitude of Shallow Earthquakes," *Bull. Seism. Soc. Am.*, 35: 57–69 (1945).
8. Gutenberg, B., "Magnitude Determination for Deep-Focus Earthquakes," *Bull. Seism. Soc. Am.*, 35: 117–130 (1945).
9. Gutenberg, B., "Amplitudes of Surface Waves and Magnitudes of Shallow Earthquakes," *Bull. Seism. Soc. Am.*, 35: 3–12 (1945).
10. Gutenberg, B., and C. F. Richter, "On Seismic Waves, Fourth Paper," *Gerlands Beitr. z. Geophys.*, 54: 94–136 (1939).
11. Gutenberg, B., and C. F. Richter, "Materials for the Study of Deep-Focus Earthquakes," first paper, *Bull. Seism. Soc. Am.*, 26: 341–390 (1936); second paper, *ibid.*, 27: 157–183 (1937).
12. Gutenberg, B., and C. F. Richter, "Earthquake Magnitude, Intensity, Energy and Acceleration," *Bull. Seism. Soc. Am.*, 32: 163–191 (1942).
13. Gutenberg, B., and C. F. Richter, *Seismicity of the Earth and Associated Phenomena* (Princeton University Press, 1949).
14. Martner, S. T., "Observation on Seismic Waves Reflected at the Core Boundary of the Earth," unpubl. diss., California Institute of Technology, Pasadena (1948); the same in condensed form, *Bull. Seism. Soc. Am.*, 40: 95–109 (1950).
15. Richter, C. F., "An Instrumental Earthquake Magnitude Scale," *Bull. Seism. Soc. Am.*, 25: 1–32 (1935).
16. Mooney, H. M., "A Study of the Energy Contained in the Seismic Waves P and pP," unpubl. diss., California Institute of Technology, Pasadena (1950); the same in condensed form, *Bull. Seism. Soc. Am.*, 41: 13–32 (1951).
17. Rudzki, M. P., "Parametrische Darstellung der elastischen Wellen in anisotropen Medien," *Publ. Acad. des Sciences de Cracovie*, Okt. (1911), pp. 503–536; an Abstract of the same paper in German, in *Gerlands Beitr. z. Geophys.*, Kleine Mitteilungen, 11–12; 75–79 (1911–1913).
18. Stoneley, R., "The Seismological Implications of Aeolotropy in Continental Structure," *Mon. Not. Roy. Astron. Soc., Geophys. Suppl.*, 5: 343–353 (1949).
19. Zoeppritz, K., L. Geiger, and B. Gutenberg, "Ueber Erdbebenwellen. V," *Nach. d. k. Ges. d. Wiss. z. Göttingen*, math.-phys. Kl., pp. 121–206 (1912).

CALIFORNIA INSTITUTE OF TECHNOLOGY
PASADENA, CALIFORNIA
(Division of the Geological Sciences, Contribution no. 549)